Ⓔ

STEPS TOWARD DETERMINATION OF THE SIZE AND STRUCTURE OF THE BROAD-LINE REGION IN ACTIVE GALACTIC NUCLEI. XVI. A 13 YEAR STUDY OF SPECTRAL VARIABILITY IN NGC 5548

B. M. Peterson,[1] P. Berlind,[2] R. Bertram,[1,3] K. Bischoff,[4] N. G. Bochkarev,[5] N. Borisov,[6] A. N. Burenkov,[6,7] M. Calkins,[2] L. Carrasco,[8] V. H. Chavushyan,[8] R. Chornock,[9] M. Dietrich,[10] V. T. Doroshenko,[11] O. V. Ezhkova,[12] A. V. Filippenko,[9] A. M. Gilbert,[9] J. P. Huchra,[2] W. Kollatschny,[4] D. C. Leonard,[9,13] W. Li,[9] V. M. Lyuty,[11] Yu. F. Malkov,[14] T. Matheson,[2,9] N. I. Merkulova,[7,14] V. P. Mikhailov,[6] M. Modjaz,[2,9] C. A. Onken,[1] R. W. Pogge,[1] V. I. Pronik,[7,14] B. Qian,[15] P. Romano,[1] S. G. Sergeev,[7,14] E. A. Sergeeva,[7,14] A. I. Shapovalova,[6,7] O. I. Spiridonova,[6] J. Tao,[15] S. Tokarz,[2] J. R. Valdes,[8] V. V. Vlasiuk,[6] R. M. Wagner,[1,3] AND B. J. Wilkes[2]

ABSTRACT

We present the final installment of an intensive 13 year study of variations of the optical continuum and broad Hβ emission line in the Seyfert 1 galaxy NGC 5548. The database consists of 1530 optical continuum measurements and 1248 Hβ measurements. The Hβ variations follow the continuum variations closely, with a typical time delay of about 20 days. However, a year-by-year analysis shows that the magnitude of emission-line time delay is correlated with the mean continuum flux. We argue that the data are consistent with the simple model prediction between the size of the broad-line region and the ionizing luminosity, $r \propto L_{\mathrm{ion}}^{1/2}$. Moreover, the apparently linear nature of the correlation between the Hβ response time and the nonstellar optical continuum F_{opt} arises as a consequence of the changing shape of the continuum as it varies, specifically $F_{\mathrm{opt}} \propto F_{\mathrm{UV}}^{0.56}$.

Subject headings: galaxies: active — galaxies: individual (NGC 5548) — galaxies: nuclei — galaxies: Seyfert

On-line material: machine-readable table

[1] Department of Astronomy, Ohio State University, 140 West 18th Avenue, Columbus, OH 43210–1173; peterson@astronomy.ohio-state.edu, onken@astronomy.ohio-state.edu, pogge@astronomy.ohio-state.edu, promano@astronomy.ohio-state.edu.

[2] Harvard-Smithsonian Center for Astrophysics, 60 Garden Street, Cambridge, MA 02138; pberlind@cfa.harvard.edu, huchra@cfa.harvard.edu, tmatheson@cfa.harvard.edu, mmodjaz@cfa.harvard.edu, belinda@cfa.harvard.edu.

[3] Mailing address: Steward Observatory, University of Arizona, Tucson, AZ 85721; rayb@as.arizona.edu, rmw@as.arizona.edu.

[4] Universitäts-Sternwarte Göttingen, Geismarlandstr. 11, D–37083 Göttingen, Germany; bischoff@uni-sw.gwdg.de, wkollat@gwdg.de.

[5] Sternberg Astronomical Institute, Lomonosov Moscow State University, Universitetskij Prosp. 13, Moscow 119992, Russia; boch@sai.msu.ru.

[6] Special Astrophysical Observatory, Russian Academy of Sciences, Nizhnij Arkhyz, Karachai-Cherkess Republic, 357147, Russia; ban@sao.ru, mvp@sao.ru, ospir@sao.ru, ashap@sao.ru, ospir@sao.ru, vvlas@sao.ru.

[7] Isaac Newton Institute of Chile, Special Astrophysical Observatory Branch and Crimean Branch.

[8] Instituto Nacional de Astrofisica, Optica y Electronica, Apartado Postal 51, CP 72000, Puebla, Mexico; carrasco@inaoep.mx, vahram@inaoep.mx, jvaldes@inaoep.mx.

[9] Department of Astronomy, University of California, Berkeley, CA 94720–3411; rchornock@astro.berkeley.edu, alex@astro.berkeley.edu, agilbert@astro.berkeley.edu, wli@astro.berkeley.edu.

[10] Department of Astronomy, University of Florida, 211 Bryant Space Science Center, Gainesville, FL 32611–2055; dietrich@astro.ufl.edu.

[11] Crimean Laboratory of the Sternberg Astronomical Institute, p/o Nauchny, Crimea, 98409, Ukraine; doroshen@sai.crimea.ua, lyuty@sai.crimea.ua.

[12] Ulugbek Astronomical Institute, Academy of Science of Uzbekistan, Astronomicheskaya ul. 33, Tashkent, 700052, Uzbekistan; oezh@sai.msu.ru.

[13] Current address: Department of Astronomy, University of Massachusetts, Amherst, MA 01003-9305; leonard@nova.astro.umass.edu.

[14] Crimean Astrophysical Observatory, P/O Nauchny, 98409 Crimea, Ukraine; nelly@astro.crao.crimea.ua, vpronik@crao.crimea.ua, sergeev@crao.crimea.ua, selena@crao.crimea.ua.

[15] Shanghai Astronomical Observatory, Shanghai 200030, China; taojun@center.shao.ac.cn.

1. INTRODUCTION

The nature of the broad-line region (BLR) is arguably one of the major remaining mysteries in active galactic nuclei (AGNs). Whereas the supermassive black hole/accretion disk paradigm has become increasingly more secure, there is still no consensus about the origin of the broad emission lines that are prominent features of the UV/optical spectra of these sources. This is not to say that progress has not been made. Years of spectroscopic study have uncovered a rich phenomenology (see Sulentic, Marziani, & Dultzin-Hacyan 2000 for a recent review).

Of particular importance has been the recognition that the emission-line fluxes vary in response to continuum variations, with a small time delay (days to weeks for Seyfert galaxies) due to light-travel time effects within the BLR. Well before these time delays were first accurately measured, this led to the seminal paper on "reverberation mapping" (Blandford & McKee 1982), a tomographic method of determining the structure and kinematics of the BLR. While the full potential of reverberation mapping has yet to be realized, use of this technique has provided BLR sizes in approximately three dozen AGNs (see compilations by Wandel, Peterson, & Malkan 1999 and Kaspi et al. 2000). Even more importantly, measurement of the emission-line time delays (or "lags"), combined with measurements of the line width, have led to estimates of the masses of the central black holes.

In late 1988, we began a program of spectroscopic monitoring of optical variations in the Seyfert 1 galaxy NGC 5548. This activity was organized by an informal consortium called the "International AGN Watch" (Alloin et al. 1994; Peterson 1999). Initially, the optical monitoring program was undertaken in support of an

TABLE 1
Summary of Program on NGC 5548

Year (1)	Dates (2)	Comments (3)	References (4)
1............	1988 Dec 14–1989 Aug 7	UV continuum and lines	1
	1988 Dec 14–1989 Oct 10	Optical continuum and Hβ	2
		Multiple optical lines	3
		Balmer continuum and Fe II	4
		Optical imaging/photometry	5
		Revised optical continuum	6
2............	1989 Dec 1–1990 Oct 15	Optical continuum and Hβ	6
3............	1990 Nov 29–1991 Oct 5	Optical continuum and Hβ	7
4............	1992 Jan 1–Oct 3	Optical continuum and Hβ	7
5............	1993 Mar 14–May 27	UV continuum and lines	8
	1992 Nov 27–1993 Sep 25	Optical continuum and Hβ	8
	1993 Mar 10–May 14	EUV continuum	9
6............	1993 Nov 17–1994 Oct 11	Optical continuum and Hβ	10
7............	1994 Nov 22–1995 Oct 17	Optical continuum and Hβ	10
8............	1995 Nov 22–1996 Oct 16	Optical continuum and Hβ	10
		Revised optical continuum and Hβ	11
9............	1996 Dec 17–1997 Oct 7	Optical continuum and Hβ	11
10..........	1997 Nov 22–1998 Sep 28	Optical continuum and Hβ	11
11..........	1998 Nov 24–1999 Oct 4	Optical continuum and Hβ	11
12..........	1999 Dec 5–2000 Sep 3	Optical continuum and Hβ	11
13..........	2000 Nov 30–2001 Dec 21	Optical continuum and Hβ	11

References.—(1) Paper I. (2) Paper II. (3) Dietrich et al. 1993 (Paper IV). (4) Maoz et al. 1993. (5) Romanishin et al. 1995. (6) Paper III. (7) Paper VII. (8) Paper VIII. (9) Marshall et al. 1997. (10). Paper XV. (11). This work.

ultraviolet monitoring campaign carried out with the *International Ultraviolet Explorer* (*IUE*; Clavel et al. 1991, the first paper in the same series as this work and hereafter referred to as Paper I). The resulting optical data set (Peterson et al. 1991, hereafter Paper II) proved to be so rich that it was decided to continue this program. Since that time, a number of additional contributions to this series (Peterson et al. 1992, hereafter Paper III; Peterson et al. 1994, hereafter Paper VII; Korista et al. 1995, hereafter Paper VIII; Peterson et al. 1999, hereafter Paper XV) have described our continuing optical monitoring program. A complete summary of the work on NGC 5548 by this consortium appears in Table 1. Reviews of the progress of this program are also available (see, e.g., Peterson 1993, 2001; Netzer & Peterson 1997).

This paper represents the final installment of our 13 year program of optical monitoring of NGC 5548. As is customary for the papers in this series, we will focus primarily on the data and the salient results of cross-correlation analysis of the continuum and emission-line light curves. Further in-depth analysis will be left to subsequent papers. In § 2, we describe the observations, data reduction, and intercalibration procedures that we have used to construct a homogeneous database of optical continuum and Hβ emission-line fluxes. In § 3, we describe the time series analysis that we have undertaken to determine the timescale for response of Hβ to continuum variations. In § 4, we discuss some of the implications of our study. Our results are summarized in § 5. We also note that some of the data presented here have already appeared in other contexts, specifically as part of a short but intensive monitoring program carried out in 1998 June (Dietrich et al. 2001) and as part of a long-term photometric monitoring campaign (Doroshenko et al. 2001).

2. OBSERVATIONS AND DATA ANALYSIS

2.1. *Spectroscopic Observations*

Here we analyze spectroscopic observations made between 1995 November 22 (Julian date = JD 2,450,044) and 2001 September 21 (JD 2,452,174); UT dates are used throughout this paper. During this 6 year period, a total of 543 individual spectra were obtained, as summarized in Table 2. Column (1) gives a code for each data set; these are the same codes that have been used throughout the NGC 5548 monitoring project. A more complete log of observations, as has been published in our previous papers on NGC 5548, can be found at the International AGN Watch Web site.[16]

The data obtained during year 8 of this program (see Table 1) were previously published in Paper XV. Here we completely reanalyze the data from year 8 because 46 additional spectra from set F have become available to us since Paper XV was published.[17]

The spectroscopic images were processed by individual observers in standard fashion for CCD frames, including bias subtraction, flat-field correction, wavelength calibration, and flux calibration based on standard-star observations. The flux calibration is then refined by scaling each spectrum to a constant value of the [O III] λ5007 narrow-line

---

[16] The light curves and complete logs of observation are available in tabular form at http://www.astronomy.ohio-state.edu/~agnwatch. All publicly available International AGN Watch data can be accessed at this site, which also includes complete references to published AGN Watch papers.

[17] We also note in passing that we have included in the AGN Watch archive five additional set H spectra from years 3 and 4 (details are provided on the AGN Watch Web site), although these data have not been incorporated into the light curves that are currently available.

TABLE 2
Sources of Spectroscopic Observations, Years 8–13

Data Set (1)	Telescope and Instrument (2)	Number of Spectra (3)
A..............	1.8 m Perkins Telescope+Ohio State CCD Spectrograph	57
F	1.5 m Mount Hopkins Telescope+CCD Spectrograph	258
GH	2.1 m Guillermo Haro Observatory Telescope+B&C Spectrograph	22
H	3.0 m Lick Shane Telescope+Kast Spectrograph	28
K	2.4 m MDM Observatory Hiltner Telescope+MODSPEC Spectrograph	6
L	6 m Special Astrophysical Observatory Telescope+CCD Spectrographs	19
L1	1 m Special Astrophysical Observatory Telescope+CCD Spectrographs	32
M.............	3.5 and 2.2 m Calar Alto Telescopes+CCD Spectrograph	7
R..............	1.5 m Loiano Telescope+CCD Spectrograph	1
W.............	2.6 m Shajn Telescope+CCD Spectrograph	113
Total		543

flux, as we have done in each previous paper in this series. All spectra are gray scaled in flux (i.e., adjusted by a constant multiplicative factor) to a constant flux of $F([\text{O iii}]\lambda 5007) = 5.58 \times 10^{-13}$ ergs s^{-1} cm^{-2}. This absolute flux was determined from spectra made under photometric conditions during the first year of this program (Paper II). Scaling is accomplished automatically by use of the van Groningen & Wanders (1992) spectral scaling software, as described in Paper XV.

After flux scaling, measurements of each of the spectra are made. The continuum flux at $\sim$5100 Å (in the rest frame of NGC 5548, $z = 0.0167$) is determined by averaging the flux in the 5185–5195 Å bandpass (in the observed frame). The Hβ emission-line flux is measured by assuming a linear underlying continuum between $\sim$4790 and $\sim$5170 Å and integrating the flux above this continuum between 4795 and 5018 Å (all wavelengths in the observed frame). The long-wavelength cutoff of this integration band misses some of the Hβ flux underneath [O iii] λ4959 but avoids the need to estimate the Fe ii contribution to this feature and still gives a good representation of the Hβ variability. We also note that no attempt has been made to correct for contamination of the line measurement by the *narrow-line* component of Hβ, which is of course expected to be constant.

Even after scaling all of the spectra to a common value of the [O iii] λ5007 flux, there are systematic differences between the light curves produced from data obtained at different telescopes. As in our previous papers, we correct for the small offsets between the light curves from different sources in a simple, but effective, fashion. We attribute these small relative offsets to aperture effects (Peterson et al. 1995), although the procedure we use also corrects for other unidentified systematic differences between data sets. We define a point-source correction factor φ by the equation

$$F(\text{H}\beta)_{\text{true}} = \varphi F(\text{H}\beta)_{\text{observed}} . \qquad (1)$$

This factor accounts for the fact that different apertures result in different amounts of light loss for the point-spread function (which describes the surface brightness distribution of both the broad lines and the AGN continuum source) and the partially extended narrow-line region.

After correcting for aperture effects on the point-spread function to narrow-line ratio, we also correct for the

different amounts of starlight admitted by different apertures. An extended source correction G is thus defined as

$$F_\lambda(5100 \text{ Å})_{\text{true}} = \varphi F_\lambda(5100 \text{ Å})_{\text{observed}} - G . \qquad (2)$$

Intercalibration of the individual data sets is then accomplished by comparing pairs of nearly simultaneous observations from different data sets to determine for each data set the values of the constants φ and G that are needed to adjust the emission-line and continuum fluxes to a common scale. Furthermore, the formal uncertainties in φ and G reflect the uncertainties in the individual data sets, so we can determine the nominal uncertainties for each data set if we assume that the errors add in quadrature.

As in our previous work, the data are adjusted relative to data set A because these data are fairly extensive, overlap well with most of the other data sets, and were obtained through a reasonably large aperture ($5''.0 \times 7''.5$). As in Paper XV, fractional uncertainties of $\sigma_{\text{cont}}/F_\lambda(5100 \text{ Å}) \approx 0.020$ and $\sigma_{\text{line}}/F(\text{H}\beta) \approx 0.020$ for the continuum and Hβ line, respectively, are adopted for the similar, large-aperture, high-quality data sets A and H, based on the differences between closely spaced observations within these sets (see also Peterson et al. 1998a). For the other data sets, it was possible to estimate the mean uncertainties in the measurements by comparing them to measurements from other sets for which the uncertainties are known and by assuming that the uncertainties for each set add in quadrature.

The intercalibration constants we use for each data set are given in Table 3, and these constants are used with equations (1) and (2) to adjust the spectral measurements. We note that there were a few cases in which the intercalibration constants had to be evaluated on a year-to-year basis to effect an acceptable intercalibration with the rest of the data.

2.2. *Photometric Observations*

In addition to the spectroscopic observations, numerous *V*-band photometric observations of NGC 5548 were made. The sources of these observations are summarized in Table 4, and a more complete log of observations is available on the AGN Watch Web site. Many of the observations used in this analysis were also included in a study by Doroshenko et al. (2001).

TABLE 3
FLUX-SCALE FACTORS FOR OPTICAL SPECTRA

Data Set (1)	Point-Source Scale Factor φ (2)	Extended Source Correction G ($\times 10^{-15}$ ergs s^{-1} cm^{-2} Å^{-1}) (3)
A............................	1.000	0.000
F (year 8)...............	0.941 ± 0.035	-1.730 ± 0.050
F (years 9–13)........	1.039 ± 0.042	-0.532 ± 0.570
GH	0.985 ± 0.032	-0.329 ± 0.555
H	1.013 ± 0.044	-0.418 ± 0.404
K	1.010 ± 0.050	0.234 ± 0.448
L	1.003 ± 0.056	-0.874 ± 0.645
L1 (year 10)...........	1.113 ± 0.045	4.088 ± 0.396
L1 (year 11)...........	1.011 ± 0.024	1.500 ± 0.931
L1 (year 12)...........	1.054 ± 0.064	2.556 ± 0.844
L1 (year 13)...........	1.011 ± 0.094	3.090 ± 0.954
M...........................	0.990 ± 0.014	-1.353 ± 0.380
R............................	0.863 ± 0.025	-1.900 ± 1.065
W (year 8)	0.932 ± 0.031	-1.319 ± 0.437
W (years 9–13)	1.009 ± 0.022	-0.422 ± 0.244

In order to effect an intercalibration with the spectroscopic light curve, we compared closely spaced pairs of spectroscopic and photometric observations and performed a least-squares fit to the equation,

$$F_\lambda(5100 \text{ Å}) = a + bF_V \ , \qquad (3)$$

where the magnitude $V \propto -2.5 \log F_V$. This fit was based on pairs of observations obtained within 1 day of each other. The raw V-band fluxes were adjusted using equation (3) to the $F_\lambda(5100 \text{ Å})$ scale defined by the spectrophotometry.

2.3. The Merged Light Curves

A complete continuum light curve was assembled by merging the spectrophotometric and V-band photometric light curves described above. The final light curves for the optical continuum and Hβ fluxes were then constructed by computing a weighted average of points separated in time by less than 0.1 days. The final light curves for years 8–13 are given in Table 5. It is important to note that all measurements are in the observer's frame and are uncorrected for Galactic extinction. Also, the continuum flux includes a contribution from the host galaxy, which we estimate to be 3.4×10^{-15} ergs s^{-1} cm^{-2} Å^{-1} (Romanishin et al. 1995), and the emission-line flux includes the narrow-line component, which we estimate to be $\sim 8.2 \times 10^{-14}$ ergs s^{-1} cm^{-2} (Wanders & Peterson 1996); both of these values are in the observer's reference frame.

3. VARIABILITY ANALYSIS

The data given in Table 5 can be combined with our previously published light curves (Papers II, III, VII, VIII, and XV), yielding homogeneous light curves that cover a span of 4756 days. The combined data are shown in Figure 1. These light curves are comprised of 1530 continuum measurements and 1248 line measurements. In this section, we will summarize the basic characteristics of the 13 year homogeneous database.

TABLE 4
SOURCES OF PHOTOMETRIC OBSERVATIONS, YEARS 9–13

Data Set (1)	Telescope and Instrument (2)	Number of Observations (3)
A.................	0.6 m Telescope, Crimean Laboratory of the Sternberg Astronomical Institute+pulse-counting UBV photometer, 14″.3 aperture	91
B	1.25 m Telescope, Crimean Astrophysical Observatory+pulse-counting Photometer-Polarimeter, 15″ aperture	12
C	1.56 m Telescope, Shanghai Astronomical Observatory+CCD, 10″ aperture	7
D	0.48 and 0.6 m Telescopes of Ulugbek Astronomical Institute+pulse-counting UBV photometer, 14″.3 aperture	69
E	1 and 0.6 m Telescopes of the Special Astrophysical Observatory+CCD, 10″ aperture	67
Total		246

TABLE 5
Optical Continuum and Hβ Light Curves

Julian Date (−2,400,000) (1)	$F_\lambda(5100 \text{ Å})$ ($\times 10^{-15}$ ergs s^{-1} cm^{-2} Å^{-1}) (2)	$F(\text{H}\beta)$ ($\times 10^{-13}$ ergs s^{-1} cm^{-2}) (3)
50,044.05....................	11.52 ± 0.23	9.56 ± 0.19
50,048.60....................	10.97 ± 0.49	8.78 ± 0.23
50,052.08....................	10.77 ± 0.27	8.96 ± 0.31
50,053.01....................	10.33 ± 0.21	9.02 ± 0.18
50,061.02....................	8.56 ± 0.17	9.19 ± 0.18
50,064.60....................	8.20 ± 0.37	8.33 ± 0.22
50,069.09....................	8.18 ± 0.20	8.22 ± 0.29
50,074.00....................	8.18 ± 0.33	7.27 ± 0.20
50,075.00....................	8.30 ± 0.33	7.04 ± 0.20
50,078.00....................	8.15 ± 0.33	6.92 ± 0.19

Note.—Table 5 is published in its entirety in the electronic edition of the *Astrophysical Journal*. A portion is shown here for guidance regarding its form and content.

3.1. *Characteristics of the Database*

In Tables 6 and 7, we provide a summary of the basic characteristics of the continuum and Hβ emission-line light curves, respectively, as shown in Figure 1. Column (1) indicates the subset considered, with time ranges as defined in Table 1. The number of observations in each subset is given in column (2), and columns (3) and (4) give the average and median intervals, respectively, between successive observations. The mean and rms fluxes, $F_\lambda(5100 \text{ Å})$ in Table 6 and $F(\text{H}\beta)$ in Table 7, are shown in column (5). Two standard measures of variability, F_{var} and R_{max}, are given in columns (6) and (7), respectively. The parameter F_{var} is the rms fractional variability, corrected for measurement error, as defined by Rodríguez-Pascual et al. (1997), and R_{max} is simply the ratio of maximum to minimum flux. Both of these parameters are affected by contamination of the measured
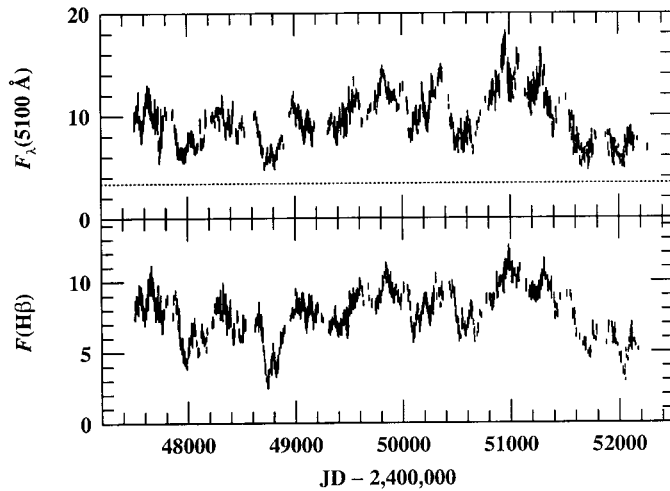

Fig. 1.—Optical continuum (*upper panel*) and Hβ (*lower panel*) light curves from 1989 December to 2001 December. The data are comprised of 1530 continuum measurements and 1248 emission-line measurements. The continuum fluxes are in units of 10^{-15} ergs s^{-1} cm^{-2} Å^{-1} and the line fluxes are in units of 10^{-13} ergs s^{-1} cm^{-2}. The horizontal dashed line is an estimate of the continuum contribution from the host galaxy (Romanishin et al. 1995) through the standard aperture used here (5″0 × 7″5). Flux measurements are in the observer's reference frame and are uncorrected for Galactic extinction.

quantities by constant-flux components, namely, the underlying host galaxy in the case of the continuum and the narrow Hβ emission component in the case of the line. If we use the values for the host galaxy contribution and the narrow-line Hβ flux given in the last section, the values of F_{var} increase to 0.380 and 0.242 for the continuum and Hβ line, respectively, and the values of R_{max} increase to 9.44 ± 1.41 and 6.26 ± 0.62, respectively. It is notable that the optical nonstellar continuum in NGC 5548 has varied by an order of magnitude over this 13 year monitoring program.

3.2. *Time Series Analysis*

As in Paper XV and previous papers, we compute the time delay between continuum variations and the Hβ response by cross-correlation of the continuum and emission-line light curves. We perform the cross-correlation analysis in two ways, using the interpolation cross-correlation function (ICCF) method of Gaskell & Sparke (1986) and Gaskell & Peterson (1987) and the discrete correlation function (DCF) method of Edelson & Krolik (1988). In both cases, we use the implementation described by White & Peterson (1994).

The results of the cross-correlation analysis are shown in Figure 2 and summarized in Table 8. The entries in Table 8 give the subset used in the analysis (col. [1]), the centroid τ_{cent} of the ICCF (col. [2]), the peak τ_{peak} of the ICCF (col. [3]), and r_{max}, the value of the ICCF at τ_{peak}. The value of τ_{cent} is computed using only those points near the principal peak with values exceeding $0.8 r_{max}$. The uncertainties quoted for τ_{cent} and τ_{peak} have been computed using the model-independent FR/RSS Monte Carlo method described by Peterson et al. (1998b).

4. DISCUSSION

It was noted in Paper XV that statistically significant year-to-year changes in the Hβ lag have occurred and that these changes are correlated with the mean continuum flux. The additional data described here confirm this result and allow us to investigate it further. In Figure 3, we plot τ_{cent} as a function of the mean starlight-corrected continuum flux for each year $\bar{F}_{opt} = \langle F_\lambda(5100 \text{ Å}) \rangle - F_{gal}$, where F_{gal} is our best estimate of the host galaxy starlight contribution

TABLE 6
SAMPLING STATISTICS FOR OPTICAL CONTINUUM

| SUBSET (1) | NUMBER OF EPOCHS (2) | SAMPLING INTERVAL (days) | | MEAN FLUX ($\times 10^{-15}$ ergs s^{-1} cm^{-2} Å^{-1}) (5) | $F_{\rm var}$ (6) | $R_{\rm max}$ (7) |
		Average (3)	Median (4)			
All data	1530	3.1	1.0	9.73 ± 2.44	0.247	3.57 ± 0.18
Year 1 (1989)........	125	2.4	1.0	9.92 ± 1.26	0.117	2.16 ± 0.16
Year 2 (1990)........	94	3.4	2.0	7.25 ± 1.00	0.129	1.82 ± 0.09
Year 3 (1991)........	65	4.8	3.0	9.40 ± 0.93	0.090	1.51 ± 0.09
Year 4 (1992)........	83	3.4	2.0	6.72 ± 1.17	0.168	2.04 ± 0.10
Year 5 (1993).........	174	1.3	0.7	9.04 ± 0.90	0.092	1.65 ± 0.08
Year 6 (1994)........	135	2.4	1.0	9.76 ± 1.10	0.104	1.76 ± 0.12
Year 7 (1995).........	83	4.0	1.9	12.09 ± 1.00	0.079	1.48 ± 0.04
Year 8 (1996..........	144	2.3	1.0	10.56 ± 1.64	0.150	1.86 ± 0.11
Year 9 (1997).........	126	2.4	1.0	8.12 ± 0.91	0.105	1.84 ± 0.06
Year 10 (1998).......	175	1.8	0.6	13.47 ± 1.45	0.100	1.59 ± 0.09
Year 11 (1999).......	148	2.1	1.0	11.83 ± 1.82	0.149	1.98 ± 0.11
Year 12 (2000).......	94	2.9	1.0	6.98 ± 1.20	0.166	2.40 ± 0.12
Year 13 (2001).......	84	4.6	2.0	7.03 ± 0.86	0.112	1.68 ± 0.10

TABLE 7
SAMPLING STATISTICS FOR Hβ EMISSION LINE

| SUBSET (1) | NUMBER OF EPOCHS (2) | SAMPLING INTERVAL (days) | | MEAN FLUX ($\times 10^{-13}$ ergs s^{-1} cm^{-2}) (5) | $F_{\rm var}$ (6) | $R_{\rm max}$ (7) |
		Average (3)	Median (4)			
All data	1248	3.7	1.1	7.82 ± 1.71	0.216	4.60 ± 0.34
Year 1 (1989)........	132	2.3	1.0	8.62 ± 0.85	0.091	1.57 ± 0.12
Year 2 (1990)........	94	3.4	2.0	5.98 ± 1.17	0.191	2.30 ± 0.12
Year 3 (1991)........	65	4.8	3.0	7.46 ± 0.81	0.093	1.58 ± 0.14
Year 4 (1992)........	83	3.4	2.0	4.96 ± 1.44	0.284	3.03 ± 0.30
Year 5 (1993)........	142	2.1	1.0	7.93 ± 0.53	0.057	1.40 ± 0.06
Year 6 (1994)........	128	2.6	1.0	7.58 ± 0.94	0.117	1.57 ± 0.07
Year 7 (1995)........	78	4.2	2.1	9.27 ± 0.70	0.071	1.38 ± 0.06
Year 8 (1996)........	144	2.3	1.0	7.95 ± 0.87	0.106	1.76 ± 0.08
Year 9 (1997)........	95	3.1	1.1	7.41 ± 0.95	0.125	1.66 ± 0.07
Year 10 (1998).......	119	2.6	1.0	10.27 ± 1.03	0.097	1.50 ± 0.07
Year 11 (1999).......	86	3.7	1.0	9.34 ± 0.61	0.058	1.50 ± 0.06
Year 12 (2000).......	37	7.6	3.0	6.27 ± 1.22	0.192	1.96 ± 0.07
Year 13 (2001).......	45	6.7	3.2	5.26 ± 1.12	0.208	2.33 ± 0.08

TABLE 8
CROSS-CORRELATION RESULTS

Subset (1)	$\tau_{\rm cent}$ (days) (2)	$\tau_{\rm peak}$ (days) (3)	$r_{\rm max}$ (4)
Year 1 (1989)........	$19.73^{+2.03}_{-1.40}$	$21.5^{+3.0}_{-4.1}$	0.877
Year 2 (1990)........	$19.34^{+1.86}_{-2.96}$	$18.5^{+2.0}_{-0.7}$	0.909
Year 3 (1991)........	$16.35^{+3.75}_{-3.28}$	$17.5^{+2.7}_{-5.7}$	0.740
Year 4 (1992)........	$11.37^{+2.30}_{-2.30}$	$13.7^{+0.6}_{-4.7}$	0.918
Year 5 (1993)........	$13.61^{+1.41}_{-1.91}$	$13.2^{+1.9}_{-3.3}$	0.730
Year 6 (1994)........	$15.49^{+2.26}_{-6.09}$	$8.7^{+8.5}_{-2.4}$	0.832
Year 7 (1995)........	$21.43^{+2.31}_{-3.00}$	$22.9^{+5.1}_{-3.1}$	0.880
Year 8 (1996)........	$16.56^{+1.78}_{-1.08}$	$15.3^{+1.4}_{-1.3}$	0.907
Year 9 (1997)........	$17.49^{+2.12}_{-1.74}$	$17.7^{+3.4}_{-1.8}$	0.803
Year 10 (1998).......	$26.44^{+4.67}_{-2.63}$	$31.7^{+0.5}_{-10.9}$	0.844
Year 11 (1999).......	$25.75^{+4.97}_{-3.32}$	$34.4^{+1.0}_{-18.5}$	0.846
Year 12 (2000).......	$6.12^{+4.44}_{-4.08}$	$8.0^{+5.4}_{-5.2}$	0.874
Year 13 (2001).......	$14.89^{+5.30}_{-6.87}$	$8.0^{+14.6}_{-1.4}$	0.793

through our standard aperture, 3.4×10^{-15} ergs s^{-1} cm^{-2} Å^{-1} at 5100 Å (Romanishin et al. 1995); $\bar{F}_{\rm opt}$ is thus the mean nonstellar flux from the AGN component only. We add to this a measurement from an earlier monitoring campaign at Wise Observatory (Netzer et al. 1990), adjusted as described in Paper XV. The best-fit power-law relationship between the continuum flux and time lag is $\tau_{\rm cent} \propto \bar{F}_{\rm opt}^{0.95}$, nearly a linear relationship.

This result can be compared with a simple theoretical prediction. Photoionization equilibrium models for the BLR are characterized by (1) the shape of the ionizing continuum incident on the BLR gas and (2) an ionization parameter U, which is the ratio of ionizing photon density to particle density at the cloud inner face,

$$U = \frac{Q(H)}{4\pi r^2 n_H c} , \qquad (4)$$

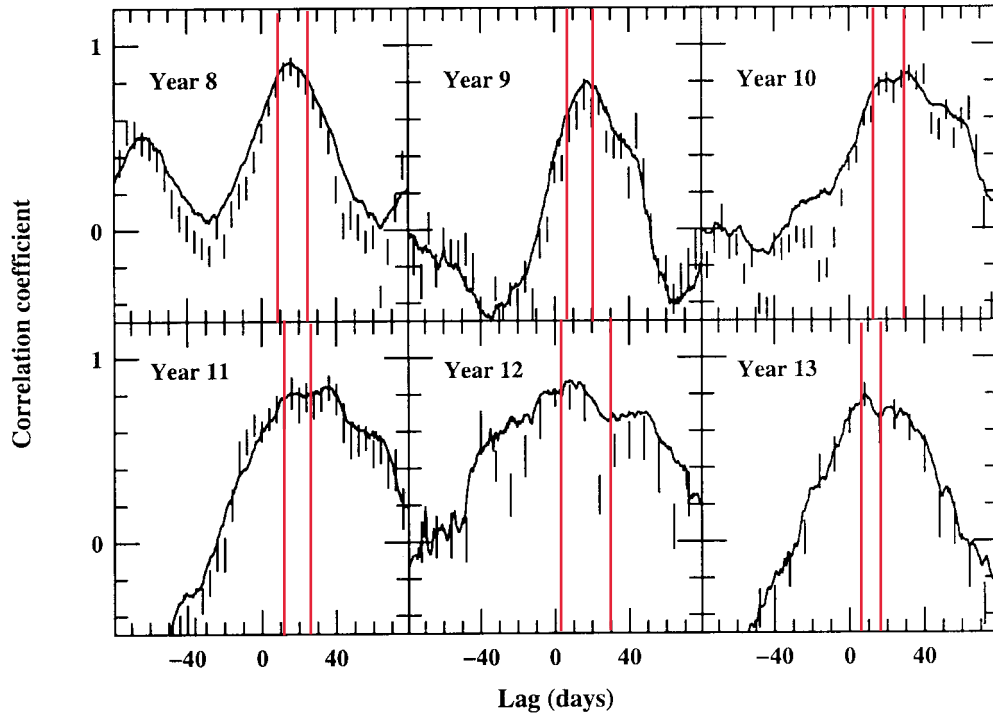where $Q(H)$ is the rate at which ionizing photons are

FIG. 2.—Cross-correlation functions for the continuum and Hβ emission-line light curves of NGC 5548. The various panels represent subsets of the new data presented here. The solid line shows the ICCF, and the vertical lines represent the 1 σ uncertainties associated with the DCF values. The peaks and centroids of the ICCFs are summarized in Table 8.

produced by the continuum source, r is the separation between the BLR gas and the continuum source, and $n_{\rm H}$ is the BLR particle density. Since the luminosity in ionizing photons $L_{\rm ion}$ is proportional to $Q({\rm H})$, we expect that $r^2 \propto L_{\rm ion}/Un_{\rm H}$. Essentially, as $L_{\rm ion}$ varies, we expect that the response in a particular emission line will be greatest at some particular value of the product $Un_{\rm H}$, which will thus lead to $r \propto L_{\rm ion}^{1/2}$ for any given line; in other words, the

FIG. 3.—Cross-correlation centroid $\tau_{\rm cent}$ as a function the yearly mean optical continuum flux $\langle F_\lambda(5100 \text{ Å})\rangle$, based on 8 years of International AGN Watch data (*filled circles*) plus 1988 data from Wise Observatory (*open circle*). The vertical dashed line indicates our best estimate of the host galaxy flux $F_{\rm gal}$ through our standard aperture. The solid line is the best-fit power law to the relationship $\tau_{\rm cent} \propto F_{\rm opt}^\alpha$, where $F_{\rm opt} = F_\lambda(5100 \text{ Å}) - F_{\rm gal}$, i.e., the nonstellar optical continuum flux. We find a best-fit slope $\alpha = 0.95$. The dotted line is the best fit to the naive prediction $\tau_{\rm cent} \propto F_{\rm opt}^{1/2}$.

response of a particular line to a continuum variation ought to be dominated by gas in which the change in emissivity is greatest. In Figure 3, we show a test of this naive prediction based on fitting an $r \propto L^{1/2}$ (i.e., $\tau_{\rm cent} \propto \bar{F}_{\rm opt}^{1/2}$) power law to these data. The resulting fit is quite poor.

The simple model above makes the implicit assumption that the continuum does not change shape as it varies. This allows us to use $L_{\rm opt}$ as a surrogate for $L_{\rm ion}$, which cannot be measured directly. However, a flux at an ultraviolet wavelength closer to the Lyman edge at 912 Å would obviously provide a better surrogate for $L_{\rm ion}$ than $L_{\rm opt}$, and such data do exist in archival form, mostly from our previous UV monitoring experiments (Papers I and VIII) on NGC 5548. We have therefore recovered the NEWSIPS-extracted *IUE* spectra of NGC 5548 obtained since late 1989 from the *IUE* Final Archive in order to effect a direct comparison of the UV and optical amplitude of continuum variability. We measured the UV continuum flux $F_{\rm UV} \equiv F_\lambda(1350 \text{ Å})$ by averaging the flux in the observed wavelength range 1370–1380 Å for all *IUE* SWP spectra obtained within 1 day of optical continuum measurements. All optical fluxes within 1 day of a UV continuum measurement were used to form a weighted average optical flux. This procedure yielded 83 pairs of UV/optical continuum measurements. We then fitted a power-law function $F_{\rm opt} \propto F_{\rm UV}^\alpha$ to these data, as shown in Figure 4, yielding a best-fit slope $\alpha = 0.56$. Combining this with the above relationship between $\tau_{\rm cent}$ and the optical continuum yields $\tau_{\rm cent} \propto F_{\rm UV}^{0.53}$, which is consistent with the simple model. We note that there is no statistically significant time delay between the UV and optical continuum variations (Peterson et al. 1998b and previous papers in this series).

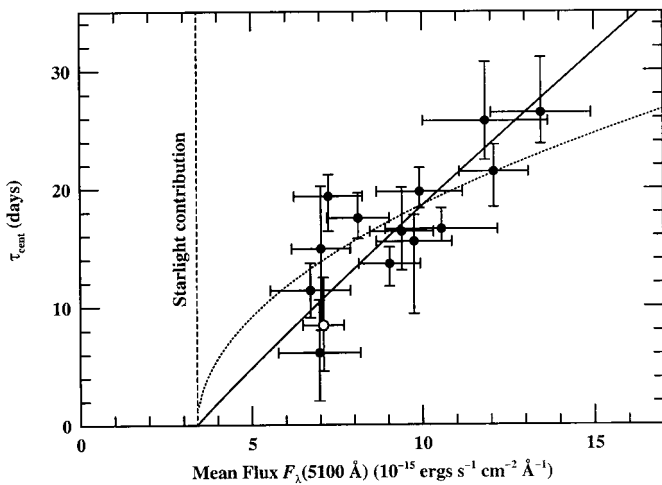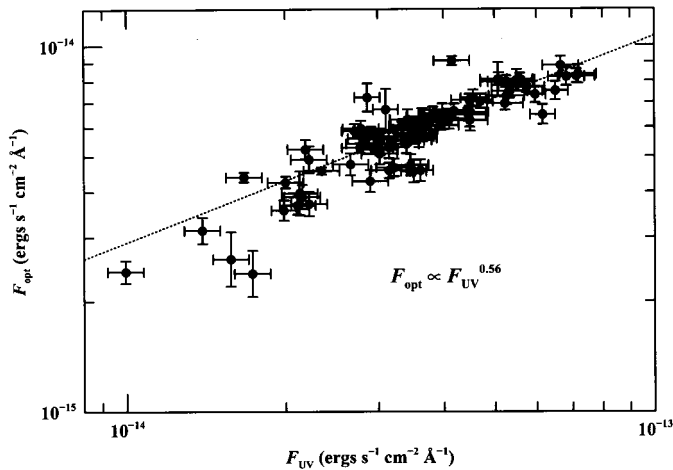Thus, the apparently linear correlation between the variations in the optical continuum and those in the Hβ emission

Fig. 4.—Relationship between UV continuum fluxes F_{UV} measured from NEWSIPS-extracted *IUE* spectra and the nonstellar optical continuum F_{opt} for pairs of UV and optical continuum measurements made within 1 day of each other. Shown as a dashed line is the best-fit power law to these data, $F_{\mathrm{opt}} \propto F_{\mathrm{UV}}^{0.56}$. Combining this relationship with that shown in Fig. 3 yields $\tau_{\mathrm{cent}} \propto F_{\mathrm{UV}}^{0.53}$, consistent with the simple model prediction $\tau_{\mathrm{cent}} \propto F_{\mathrm{UV}}^{1/2}$.

line is attributable to similar relationships between the UV and optical continuum variations on the one hand and the UV continuum and Hβ emission-line variations on the other. This probably accounts for the apparent absence of scatter (relative to, say, Lyα or C IV λ1549) in comparisons of the optical continuum and Hβ fluxes of AGNs (see, e.g., Yee 1980; Peterson 1997, pp. 90–91).

It is interesting that our observational result agrees with the naive theory once we account for the change in the shape of the continuum between the UV and optical, but that the naive theory supposes that the shape of the ionizing continuum remains unchanged. Either the shape of the continuum between the UV and extreme-ultraviolet still remains constant or the Hβ line is surprisingly insensitive to the shape of the continuum.

It should be pointed out that our result differs from the BLR radius-luminosity relationship found by Kaspi et al. (2000), namely, $r \propto L^{0.7}$. The Kaspi et al. result describes how the BLR radius varies from object to object as a function of the mean optical luminosity of the source. The relationship discussed here describes how the BLR radius in an individual object changes as the luminosity of the central source varies with time.

5. SUMMARY

We have presented an additional 5 years (1997–2001) of optical spectroscopic and photometric observations of the continuum and Hβ emission-line variations in the Seyfert 1 galaxy NGC 5548. We have also added significantly to the previously published data from 1996, warranting a complete recalibration of the data for that particular year. The new data expand our temporal coverage of variations in this AGN to a total of 1530 continuum and 1248 Hβ measurements obtained over a 4756 day span, beginning in 1988 December and terminating in 2001 December. During this period, the nonstellar optical continuum in NGC 5548 varied by approximately an order of magnitude in flux.

Analysis of the time delay between continuum variations and Hβ response allows us to confirm our earlier finding (Paper XV) that the Hβ lag varies with the mean continuum flux, ranging from a low value of $\sim$6 days in 2000 to a high value of $\sim$26 days in 1998–1999. We find consistency with the simple photoionization equilibrium prediction $\tau_{\mathrm{cent}} \propto L_{\mathrm{UV}}^{1/2}$.

REFERENCES

Alloin, D., Clavel, J., Peterson, B. M., Reichert, G. A., & Stirpe, G. M. 1994, in Frontiers of Space and Ground-Based Astronomy, ed. W. Wamsteker, M. S. Longair, & Y. Kondo (Dordrecht: Kluwer), 325
Blandford, R. D., & McKee, C. F. 1982, ApJ, 255, 419
Clavel, J., et al. 1991, ApJ, 366, 64 (Paper I)
Dietrich, M., et al. 1993, ApJ, 408, 416 (Paper IV)
———. 2001, A&A, 371, 79
Doroshenko, V. T., et al. 2001, Astron. Lett., 27, 691
Edelson, R. A., & Krolik, J. H. 1988, ApJ, 333, 646
Gaskell, C. M., & Peterson, B. M. 1987, ApJS, 65, 1
Gaskell, C. M., & Sparke, L. S. 1986, ApJ, 305, 175
Kaspi, S., Smith, P. S., Netzer, H., Maoz, D., Jannuzi, B. T., & Giveon, U. 2000, ApJ, 533, 631
Korista, K. T., et al. 1995, ApJS, 97, 285 (Paper VIII)
Maoz, D., et al. 1993, ApJ, 404, 576
Marshall, H. L., et al. 1997, ApJ, 479, 222
Netzer, H., Maoz, D., Laor, A., Mendelson, H., Brosch, N., Leibowitz, E., Almoznino, E., Beck, S., & Mazeh, T. 1990, ApJ, 353, 108
Netzer, H., & Peterson, B. M. 1997, in Astronomical Time Series, ed. D. Maoz, A. Sternberg, & E. M. Leibowitz (Dordrecht: Kluwer), 85
Peterson, B. M. 1993, PASP, 105, 247
———. 1997, An Introduction to Active Galactic Nuclei (Cambridge: Cambridge Univ. Press)

Peterson, B. M. 1999, in ASP Conf. Ser. 175, Structure and Kinematics of Quasar Broad Line Regions, ed. C. M. Gaskell, W. N. Brandt, M. Dietrich, D. Dultzin-Hacyan, & M. Eracleous (San Francisco: ASP), 49
———. 2001, in Advanced Lectures on the Starburst–AGN Connection, ed. I. Aretxaga, D. Kunth, & R. Mújica (Singapore: World Scientific), 3
Peterson, B. M., Pogge, R. W., Wanders, I., Smith, S. M., & Romanishin, W. 1995, PASP, 107, 579
Peterson, B. M., Wanders, I., Bertram, R., Hunley, J. F., Pogge, R. W., & Wagner, R. M. 1998a, ApJ, 501, 82
Peterson, B. M., Wanders, I., Horne, K., Collier, S., Alexander, T., Kaspi, S., & Maoz, D. 1998b, PASP, 110, 660
Peterson, B. M., et al. 1991, ApJ, 368, 119 (Paper II)
———. 1992, ApJ, 392, 470 (Paper III)
———. 1994, ApJ, 425, 622 (Paper VII)
———. 1999, ApJ, 510, 659 (Paper XV)
Rodríguez-Pascual, P. M., et al. 1997, ApJS, 110, 9
Romanishin, W., et al. 1995, ApJ, 455, 516
Sulentic, J. W., Marziani, P., & Dultzin-Hacyan, D. 2000, ARA&A, 38, 521
van Groningen, E., & Wanders, I. 1992, PASP, 104, 700
Wandel, A., Peterson, B. M., & Malkan, M. A. 1999, ApJ, 526, 579
Wanders, I., & Peterson, B. M. 1996, ApJ, 466, 174
White, R. J., & Peterson, B. M. 1994, PASP, 106, 879
Yee, H. K. C. 1980, ApJ, 241, 894